Agroforest Syst (2012) 84:101–116
DOI 10.1007/s10457-011-9418-z

Simple models for light competition within agroforestry discontinuous tree stands: are leaf clumpiness and light interception by woody parts relevant factors?

G. Talbot · C. Dupraz

Received: 18 October 2010 / Accepted: 6 July 2011 / Published online: 19 July 2011

Abstract Predicting the temporal and spatial variability of radiation intensity under wide-spaced tree stands is required for many applied issues in savannah-like ecosystems, orchards, agroforestry and urban forestry systems. Numerous authors have advocated the use of simple light interception models that approximate the crown shape with ellipsoids. They have suggested taking into account leaf clumping to improve the efficiency of these simple models, but this was never assessed. We tested this hypothesis together with the impact of including predictions of light interception by woody parts (trunks, branches). We calibrated and evaluated the model using cross-validation across eight walnut trees with field measurements of radiation intensity and spatial heterogeneity using hemispherical photographs. Leafless trees were efficiently modelled using Wood Area Density (WAD, m^2m^{-3}) for branches and an opaque cone for the trunk. We introduced a clumping parameter (μ) but this proved inefficient, clumping being highly variable amongst trees. This results from the limitations of representing the crown as an ellipsoid, a procedure too coarse to be improved by using a clumping parameter. The model proved efficient to predict the light pattern around an average tree, but was not fit for simulating the variability of individual trees. We finally discuss practical recommendations for modelling light competition in integrated agroforestry models simply.

Keywords Light competition · Leaf aggregation · Agroforestry model · Gap fraction · Hemispherical photographs

G. Talbot (✉) · C. Dupraz
INRA, UMR System, Bâtiment 27, 2 Place Viala,
34060 Montpellier Cedex 1, France
e-mail: talbot@supagro.inra.fr

Introduction

Wide-spaced tree stands are characteristics of many ecosystems (savannah type, opened forests) and agro-ecosystems (agroforestry, low density orchards, urban forestry). Predicting the temporal and spatial variations of radiation intensity under the tree stratum is often required when working on issues that involve a living community underneath the trees, such as understorey in forests, crops in agroforestry or grass in urban parks. Agroforestry systems are expected to spread over millions of hectares during the twentyfirst century in both temperate and tropical countries (Nair 2007; Reisner et al. 2007). Such systems are characterized by a high spatial and temporal heterogeneity, both above and below the ground (Mulia and Dupraz 2006). The productivity of both trees and the understorey is highly dependent on resource availability and competition processes. Growth patterns are co-limited by several resources simultaneously

(Kho et al. 2001). In this paper, we will focus on tree–crop mixtures, as the productivity of the crop stratum in agroforestry is central to the value of the system, and should be carefully predicted. However, the models presented here may be used for any other kind of wide-spaced trees systems.

Competition for resources in tree-crop systems evolves dynamically over time. Light competition is asymmetrical, as trees spread above crops, whereas competition for below-ground resources is more symmetrical, with intermixed root systems. The phenologies of tree and crop species are often asynchronous, resulting in various patterns of competition from day to day, season to season and year to year. Modelling these competition processes requires a daily time step to account for such dynamics. A model that could predict the productivity of tree-crop systems should be able to predict both the competition for resources and the effect of competition on tree and crop growth at the daily time step. The amount of photosynthetically active radiation (PAR) intercepted is crucial for predicting the productivity of tree and crop species. Predicting light interception by trees and spatial patterns of ground irradiance is therefore required in the dynamic modelling of such systems.

Numerous models have been proposed to simulate light interception by plant canopies (see Brunner 1998 for a review). They are usually classified according to the level of complexity of the canopy architecture. It ranges from simple, horizontally homogeneous canopies, to complex detailed descriptions at organ scale. Most of them are based on the turbid medium analogy, applying the Beer's law to predict the interception probability of a beam that crosses the canopy. The hypotheses of Beer's law in its initial formulation have been extensively discussed: (1) leaf size is to be infinitely small, and (2) leaf area density (LAD, $m^2\ m^{-3}$) uniformly and randomly distributed within the canopy volume (Sinoquet et al. 2005). Small leaf size assumption has been shown to have a negligible effect on the predictions of models for large enough plants (Thanisawanyangkura et al. 1997). But the uniform and random hypothesis for leaf area distribution may lead to an underestimation of mutual shading between leaves and consequently to overestimations of the intercepted light (Cohen et al. 1995; Begué et al. 1996; de Castro and Fetcher 1999).

Tree canopies are clumped at several scales: leaves are clumped within shoots, shoots within branches and branches within trees. Two main strategies have been proposed to account for leaf clumping. A first strategy consists of keeping a canopy description that ignores the gaps between trees, but modifies the attenuation law by introducing correcting parameters (Nilson 1971; Cohen et al. 1995). This strategy eliminates the bias of Beer's law, but is inadequate to predict the heterogeneity of PAR transmittance below trees, because canopy geometry is not described explicitly. It has been extensively used in dense forest stands for indirect estimates of the Leaf Area Index (LAI) by gap fraction inversion methods (e.g. Chen 1996). A second strategy consists of using a finer canopy geometry description. The canopy may be divided either in subvolumes corresponding to individual trees, such as ellipsoids (Norman and Welles 1983; Bartelink 1998; Martens et al. 2000), paraboloids (Courbaud et al. 2003), more complex shapes (e.g. Cescatti 1997a), eventually divided again in subvolumes (Mariscal et al. 2000) or voxels (Knyazikhin et al. 1996; de Castro and Fetcher 1998; Sinoquet et al. 2005). Leaf area distribution within subvolumes may be considered uniform or described by statistical functions (Wang and Jarvis 1990; Cescatti 1997a). Finally, some light models use an explicit stand description at scale of shoot or leaf (Dauzat et al. 2001; Mialet-Serra et al. 2001; Casella and Sinoquet 2007; Lamanda et al. 2008). The finer the level of canopy description is, the better the predictions of the models (Sinoquet et al. 2005). But both computation time and the number of input parameters increase dramatically (Mialet-Serra et al. 2001; Roupsard et al. 2008). This is not compatible with dynamic models designed for simulations over long periods of time and applied to a large number of species.

Separation between tree crowns usually is the main source of clumping (Bartelink 1998; Nilson 1999), and most light models for forest, orchard or agroforestry stands use a stand geometry description at the scale of individual trees. Each tree crown is represented by a volume assimilated to a turbid medium. This description level provides accurate predictions of transmitted light repartition at a daily time step (Norman and Welles 1983; Bartelink 1998; Mariscal et al. 2000, 2004). The transmittance of tree crowns in such models may be simulated either by a

porosity coefficient (Oyarzun et al. 2007) or by using Beer's law (e.g. Norman and Welles 1983; Courbaud et al. 2003; Zhao et al. 2003): $I = I_0 \exp(-kL)$ where I_0 and I are light intensity before and after crown crossing, L the path length within tree crown, and k the extinction coefficient. k may be estimated from experimental data (Zhao et al. 2003) or approximated as a function of leaf area density, leaf angle distribution and the optical properties of leaves. Sensitivity analyses have shown that the predictions of such models are sensitive to k (Stadt and Lieffers 2000; Zhao et al. 2003) or to the porosity parameter (Oyarzun et al. 2007).

A canopy description at the scale of individual trees explicitly accounts for leaf clumping in discrete tree crowns. It generally assumes a random dispersion of leaves within the crown. However, simple geometrical shapes are very rough approximations of real tree shapes, and leaves are clustered within shoots (Cohen et al. 1995; Falster and Welstoby, 2003). In some cases the effective leaf area density or the extinction coefficient of tree crowns may be estimated using optical methods (Zhao et al. 2003; Annandale et al. 2004), implicitly accounting for leaf clumping. In other cases, leaf area is estimated by destructive (Mariscal et al. 2000; Stadt and Lieffers 2000) or allometric methods (Cescatti 1997b; Brunner 1998), and the random hypothesis may lead to discrepancy between model predictions and experimental data (Mariscal et al. 2000).

The light interception by branches and trunks is usually ignored by forest or orchard tree growth models (but see Brunner 1998). It has no direct impact on tree growth: shading on tree leaves caused by ligneous parts of the tree is assumed to be negligible. But when the model is expected to predict light availability for the understorey, light interception by the opaque ligneous parts of trees may become significant. This is particularly crucial in temperate agroforestry comporting deciduous tree species. In these systems, many crops grow at times of the year when the tree is leafless (Dupraz and Newman 1997).

We have designed a model for light availability that will later be embedded in a dynamic biophysical model of agroforestry stands that should manage trees and crops growth at the daily time step, and integrate competition for light, water and nitrogen . This light model should meet the two following expectations: (i) a description of the shape and size of the crowns that is easy to parameterize, and (ii) fast computation speed to allow for simulating multiple trees concurrently for the whole life of the trees (century time scale). This model was inspired by the Mountain model (Courbaud et al. 2003), a ray-tracing model that uses ellipsoids or paraboloids for a simple crown description. We intend to evaluate the potential for an increased model accuracy through the introduction of simple formalisms, with a negligible impact on computation time. We explored four strategies: (1) the explicit computation of light interception by tree stems, (2) introducing wood area density (WAD, m^2m^{-3}) to account for light interception due to branches, (3) introducing an explicit leaf angle distribution in place of the spherical assumption; and (4) introducing a clumping coefficient (μ) at the scale of an individual tree crown. We propose a gap-fraction inversion method to estimate parameters μ and WAD. This method was applied to eight hybrid walnuts from two temperate agroforestry systems located in the South of France. We will discuss the relevance of the formalisms introduced by comparing the model's predictions for the shaded-fraction of sky (complementary to the gap-fraction) to estimates obtained with hemispherical photographs. The sensitivity of the model to μ and WAD is analyzed.

Materials and methods

Light competition model

Simplified stand description

The model computes daily light repartition within a rectangular plot divided in square cells. The plot may have a slope of any steepness or aspect. Each cell may host a crop, a tree, or both. Crops are assumed to be homogeneous across a cell. They are modelled using the crop model STICS (Brisson et al. 1998). The tree canopy is described at the scale of an individual tree: each crown is represented by an ellipsoid filled with foliage and considered a turbid medium.

Light models often use a torus approach to avoid artificial edge effects (Courbaud et al. 2003). The modelled plot is virtually replicated towards infinity

in all directions. This allows the simulation of an infinite tree stand. For this study, we needed to simulate an isolated tree. We designed an optional toric symmetry algorithm that permits "switching off" toric symmetry, either for the positive and/or negative side of both x- and/or y-axis. Replicates may either contain trees or not (Fig. 1a). This allows the simulation of a single tree, a hedgerow, a tree stand or the edge of a tree stand (Fig. 1b).

Incident radiation

Daily incident radiation is simulated by a finite number of beams coming from evenly distributed directions of the sky hemisphere. Each direction Ω is defined by an elevation θ and an azimuth α, and accounts for a sector of the sky vault. Daily incident radiation is shared between these sectors. Incident PAR is divided between direct and diffuse radiation using standard relationships (Bonhomme 1993). The light module predicts the % of incoming energy intercepted or transmitted and absolute values can be computed on a daily basis by applying these proportions to the absolute values of incoming energy. Diffuse radiation is shared between sections of the sky either uniformly (UOC Uniform OverCast sky radiance distribution) or according to the Standard OverCast sky (SOC, Moon and Spencer 1942). The position of the sun is computed at regular time steps using classical astronomic laws (Bonhomme 1993). For each position of the sun, direct radiation is allocated between the different sectors proportionally to the intersection area with a sector of equal solid angle centered on the sun position.

Ray-tracing method

A beam of light is calculated for each sky sector and each cell. The length of the beam's path (L) is calculated through each tree crown (see Norman and Welles 1983; Bartelink 1998; Martens et al. 2000 for details) after an optimization procedure that selects trees potentially intercepting the beam (Courbaud et al. 2003). In cases where the dimensions of a cell are large in comparison with the size of the tree, the spatial resolution of the model is increased by computing several beams per cell. Relative beam energy is decremented when it passes through crowns according to the law of attenuation. Results can then be integrated to the sky vault, to compute the daily light interception of each tree. Trunks were represented as opaque cones with a diameter DBH (Diameter at Breast Height) at 1.3 m height and a diameter of 0 at tree height.

There are two options available for modelling light interception by crops: (i) PAR transmittance below tree canopy is sky integrated and light interception by crops computed with a simple Beer's law as in

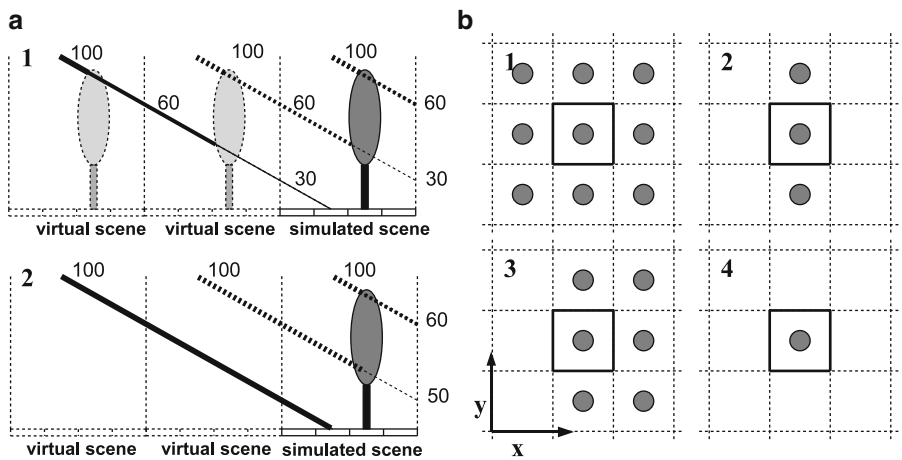

Fig. 1 Principle of the algorithm for optional toric symmetry. **a** in all cases, the simulated plot is replicated to avoid below-ground edge effects (toric symmetry), but the replicates may be either identical to the simulated plot (*1*) or void (*2*). **b** depending on the options for toric symmetry, the model can simulate an infinite stand (*1*, all replicates filled), a hedgerow (*2*, y-replicates filled), the edge of a tree stand (*3*, y and x-positive replicates filled) or a single tree (*4*, all replicates void)

conventional crop models (see Brisson et al. 1998), or (ii) competition for light between neighbour crops is accounted for by extending the ray-tracing method to crops represented by parallelepipeds. This is useful when neighbour crops have different heights.

A law for radiation interception by tree crowns

The transmittance of tree crowns is traditionally computed according to the turbid-medium analogy. We have introduced two corrections to account for leaf clumping and interception by branches. With a given ray and a given tree, gap fraction is calculated as:

$$\exp(-(G(\Omega)\mu\mathrm{LAD} + \mathrm{WAD})\mathrm{L}) \quad (1)$$

$G(\Omega)$ is the projection factor of leaf area in direction Ω (unitless), μ the clumping coefficient (unitless), LAD and WAD the leaf and wood area density ($m^2\ m^{-3}$), and L the length of the ray's path across the tree crown (m). We tested two options with the $G(\Omega)$ function: a spherical leaf angle distribution as assumed in most light models, so that $G(\Omega) = 0.5$ in all directions, and an explicit leaf angle distribution computed from measurements by Parveaud et al. (2008). A clumping coefficient below 1, equal to 1 or above 1 indicates a clumped, random or regular distribution of leaves inside the canopy volume respectively.

According to Goudriaan's approximation (1977) accounting for light scattering by leaves, the proportion of transmitted PAR is enunciated thus:

$$\frac{I}{I_0} = \exp\left(-(G(\Omega)\mu\sqrt{\sigma}\mathrm{LAD} + \mathrm{WAD})L\right) \quad (2)$$

with σ the leaf absorptance in PAR wavelength (unitless). Because the reflectance of branches and leaves is low for PAR radiation, intercepted light is considered to be complementary to transmitted light. The intercepted light is then shared between branches (with no impact on tree growth) and leaves (used for photosynthesis): we assumed that the shade of branches on tree leaves is negligible, the amount of PAR intercepted by leaves is thus given by Eq. 2 with WAD = 0. The clumping coefficient μ accounts for clumping within tree crown, i.e. leaf clumping within shoots and shoot clumping within tree crown. Clumping between separated tree crowns is imposed by the position and size of the trees on the plot, and by the procedure that calculates the size of ellipsoids. Therefore, μ depends on the procedure used to define the ellipsoids that represent tree crowns.

Optimizing the triggering of the light model

The light model is a very time consuming module of the integrated tree-crop simulation model. To reduce computation time, the module is not triggered every day, but only when either sun declination or leaf area of trees have changed significantly. In practice, with a 2° threshold for sun declination and a 5% threshold for either tree height, tree leaf area, crop height or crop leaf area, the ray-tracing method is called about 70–80 times a year.

Field estimation of the clumping index and wood area density

Tree measurements and ellipsoid calibration

We monitored eight hybrid walnut trees (*Juglans nigra x regia NJ201*), selected from two different sites (Table 1). Four trees were located in the experimental agroforestry fields at Restinclières (South of France, 43°42′N, 3° 51′E, 54 m elevation), the four others in an agroforestry plot at Notre-Dame-de-Londres (South of France, 43°49′N, 3°46′E, 160 m elevation). We selected walnut trees of various sizes (from 3.6 to 10.5 m height) and either pruned up to about 30% of total tree height or unpruned. We selected isolated trees for a simplified interpretation of hemispherical photographs.

For each tree, we measured the total height (z_{max}), the height of the lower leaf (z_{min}), and the (x, y) coordinates of the farthest leaves from the tree trunk in the four cardinal directions (x_{min},y_{min},x_{max},y_{max}). We used a simple method to define an ellipsoid from these measures (Villalobos et al. 1995): ellipsoid center coordinates are $i = (i_{max} + i_{min})/2$ and radius are $r_i = (i_{max} - i_{min})/2$, with $i = x$, y or z.

The leaf area of each tree was measured by harvesting leaves during leaf fall in October 2007. To obtain a complete gathering of tree leaves, we wrapped the trees in nets with a small mesh size before the start of leaf fall (Fig. 2), providing a measure of total leaf dry weight (W). Specific leaf area (SLA, $cm^2\ g^{-1}$) and the proportion of leaflets to the total leaf dry weight were measured prior to leaf fall in August 2007. For each tree, we sampled leaves

Table 1 Description of the monitored trees: general description: diameter at breast height (DBH); ellipsoid dimensions: coordinates of ellipsoid center relatively to plantation point (x, y, z), ellipsoid radii (r_x, r_y, r_z) and volume (V); results from leaf area measurements: average specific leaf area (SLA), leaflet to leaf dry weight proportion (p_l), total leaf dry weight (W), total leaf area (LA) and leaf area density (LAD)

General description				Ellipsoid dimensions		Leaves				
Tree name	Pruning	Height (m)	DBH (cm)	(x, y, z) (m)	(r_x, r_y, r_z) (m)	SLA ($cm^2\ g^{-1}$)	p_l (–)	W (kg)	LA (m^2)	LAD ($m^2\ m^{-3}$)
R1	No	8.2	18	(0.1, 0.13, 4.1)	(3.8, 3.7, 4.1)	98	0.80	24.5	194	0.79
R2	Yes	10.5	18.3	(− 0.2, − 1, 7)	(3.7, 2.7, 3.5)	115	0.75	13	112	0.76
R3	Yes	9.8	18.5	(0.1, 0, 6.4)	(2.9, 2.2, 3.4)	114	0.75	10.2	87	0.94
R4	No	8.4	14.2	(0.0, − 0.2, 4.6)	(3, 2.8, 3.8)	125	0.81	10.2	103	0.78
N1	No	3.6	7.3	(0.2, − 0.1, 2.4)	(1.4, 1.3, 1.2)	120	0.79	2	20	2.24
N2	No	3.8	7.6	(0.2, − 0.2, 2.7)	(1.5, 1.4, 1.1)	120	0.84	1.9	17	1.77
N3	Yes	8.3	21.1	(0.6, 0.8, 5.6)	(2.9, 3.1, 2.8)	100	0.74	18.8	140	1.34
N4	Yes	7.2	17.7	(− 0.1, 0.5, 4.6)	(2.7, 2.4, 2.5)	95	0.75	11.8	77	1.15

R Restinclières, *NDL* Notres Dame de Londres

Fig. 2 Trees were wrapped for leaf litter gathering using a mobile crane for tall trees

from the top, middle and bottom of the crown (only top and bottom for small trees), and from inside and outside the crown. Sixty leaves were collected for each tree and pinched for three 1 cm^2 round limb samples per leaf (from the distal and intermediate leaflets). The samples were oven-dried to measure the SLA of limbs. Total leaf dry-weight and rachis dry-weight were measured and used to compute the proportion (p_l) of leaflets in the leaf dry weight. This allowed us to compute the leaf area (LA) of trees as: $LA = SLA.p_l.W$.

Using hemispherical photographs to compute the gap fraction at the cell level

We shot 24 (16 for small trees) hemispherical photographs evenly distributed around each tree (Fig. 3) both in late summer (with maximal leaf area) and winter (without leaves). Neighbouring trees were erased from photographs with the Gimp software (http://www.gimp.org). The photographs were then analyzed with the Gap Light Analyser software (Frazer et al. 1999) to calculate the proportion P^{obs} of sky obscured by the tree. Because of the difficulty for separating the different trees close to the skyline, we didn't consider elevations lower than 16°.

Parameter estimation

The parameters estimation was achieved with the R statistical software (http://www.r-project.org). N = 6660 sky sectors were created at regular azimuth and elevation intervals on the sky vault with an angle

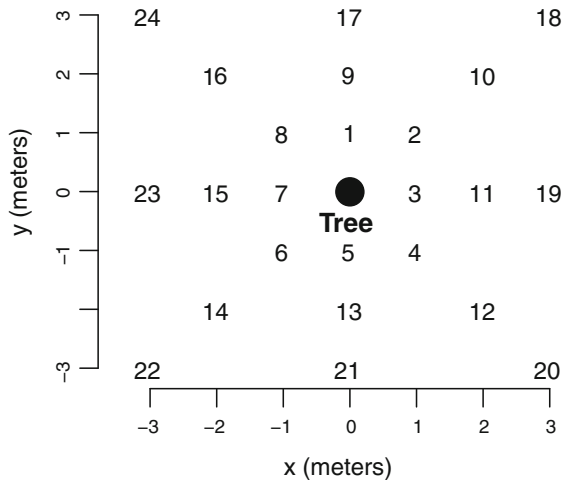

Fig. 3 Hemispherical photographs positions around trees. For all photographs, z-coordinate is 90 cm high. For the small trees N1 and N2, we limited the protocol to photographs 1–16

step of 2°, but excluding elevations under 16°. According to the law for attenuation mentioned above (Eq. 1), for each section of sky i , the simulated shaded fraction writes:

$$P_i(\mu, \mathrm{WAD}) = 1 - \exp(-(G(\Omega)\mu\mathrm{LAD} + \mathrm{WAD})L_i) \quad (3)$$

With L_i the length of the path across the tree ellipsoid of the ray coming from the sky sector i and hitting the photograph position. The simulated shaded fraction of a whole photograph is then:

$$P^{\mathrm{sim}}(\mu, \mathrm{WAD}) = \sum_{i=1}^{N} w_i P_i(\mu, \mathrm{WAD}) \quad (4)$$

with w_i the proportion of pixels on photographs situated in sector i.

Parameters were estimated with a non linear least-square regression (algorithm "nl2sol" of the PORT library—see http://www.netlib.org/port/-implemented in the nls R method) for minimizing the sum of the deviations:

$$S(\mu, \mathrm{WAD}) = \sum_{\substack{\text{seasons} \\ \text{trees} \\ \text{photographs}}} (P^{\mathrm{sim}}(\mu, \mathrm{WAD}) - P^{\mathrm{obs}})^2 \quad (5)$$

WAD was first estimated from winter photographs (LAD = 0), then μ was estimated from summer photographs.

Evaluation of the model for predicting the shaded fraction by cross-validation

The model was evaluated by computing different indices of concordance between simulated and observed (hemispherical photographs) values for the shaded fraction P: relative bias (rB), root mean squared relative error of prediction (RMSrE) and model efficiency (EF), as given by equations:

$$\mathrm{rB} = \frac{\overline{P^{\mathrm{sim}} - P^{\mathrm{obs}}}}{\overline{P}^{\mathrm{obs}}} \quad (6)$$

$$\mathrm{RMSrE} = \sqrt{\overline{\left(\frac{P^{\mathrm{sim}} - P^{\mathrm{obs}}}{P^{\mathrm{obs}}}\right)^2}} \quad (7)$$

$$\mathrm{EF} = 1 - \frac{\sum \left(P^{\mathrm{sim}} - P^{\mathrm{obs}}\right)^2}{\sum \left(\overline{P^{\mathrm{obs}}} - P^{\mathrm{obs}}\right)^2} \quad (8)$$

The efficiency provides information about the predictive power of the model relatively to the mean of the observations. When it is computed from several photographs of a same tree, it evaluates the model ability to reproduce the spatial variability of P around this tree. When it is computed from several trees, it evaluates also the model for capturing differences in P for trees of different size, shape and LAD.

To provide unbiased estimators of the indices, we used the cross-validation principles: for each tree, the model is parameterized with data from all the other trees. Summer (leafy canopies) and winter (only branches) model performances were evaluated separately.

In order to test the relevance of introducing new processes (leaf clumping, light interception by branches) we compared the model performances with and without these processes included.

Sensitivity analysis

We explored the model sensitivity to parameters μ and WAD with two virtual walnut trees, a small (5m high, $r_x = r_y = 1.9$ m, $r_z = 1.8$ m, LAD = 1.5 m^2 m^{-3}) and a large one (15 m high, $r_x = r_y = 4.5$ m, $r_z = 5.6$ m, LAD = 0.51 m^2 m^{-3}). For each tree size, a high density plot (123 tree ha^{-1}, 9 m between trees) and a low density plot (44 tree ha^{-1}, 15 m between

trees) were tested. The torus symmetry algorithm was fully activated for these simulations. We ran one year simulations with a typical phenology cycle for walnut trees: budburst on April 15th, and the end of leaf fall on November 15th. Climatic data from Restinclières, year 1997 were used, with a SOC partition for diffuse radiation. We realized simulations with μ ranging from 20 to 200% of the estimated value with a 20% step, and WAD from 0 (no branches) to 200% of the estimated value with a 20% step.

The incident PAR above the canopy is divided into three parts by the light model: PAR intercepted by tree leaves, PAR intercepted by branches and trunks, and PAR transmitted under the tree canopy. The analyzed outputs were the light capture efficiency of tree leaves, and the mean PAR transmittance below the leafy (8/3 to 23/11) or leafless (rest of the year) canopy. The light capture efficiency was computed as $\varepsilon = \mathrm{PAR_{int}}/(\mathrm{PAR_{inc}LA})$ where $\mathrm{PAR_{int}}$ is the PAR radiation intercepted by tree leaves over the year and $\mathrm{PAR_{inc}}$ the PAR incident on a unit horizontal surface above the canopy. ε is similar to the $\overline{\mathrm{STAR}}$ (Silhouette to Total Area Ratio integrated over sky vault) frequently used for isolated trees (Sinoquet et al. 2007), but integrates rediffusion (with Goudriaan's approximation) and shading between trees. The light capture efficiency has no unit, but may be expressed in $m^2\ m^{-2}$: an efficiency of 1 signifies that 1 m^2 of leaf area intercepts as much PAR as a 1 m^2 plane surface laying on the soil.

We studied the sensitivity of the model for three outputs: light capture efficiency and the summer and winter PAR transmittances. We computed their elasticity to parameters at the point defined by the nominal values for μ and WAD ($\mu = 0.76$ and WAD = 0.026) obtained after parametrization with an explicit interception by trunks and a spherical leaf angle distribution. The elasticity is defined as the ratio of the relative change in the output to the relative change in a parameter.

Results

Ellipsoid calibration

The routine for adjusting an ellipsoid to the monitored trees proved to be very easy and convenient. The center of the ellipsoids was not aligned with the trunk position for most trees (x or y different from 0), indicating asymmetrical crowns (Table 1). Small trees had very high LAD compared to large trees. For the large trees, there was no substantial relationship between the pruning regime and the LAD. We could have expected the opposite, as pruning results in irregular canopies with large empty areas inside the ellipsoid.

Parameters estimation

Estimates of the wood area density

When the interception by trunks was not explicitly computed, the estimated wood area density accounted for both trunks and branches, and ranged from 0.023 $m^2\ m^{-3}$ for tree R2 to 0.059 $m^2\ m^{-3}$ for tree N3 (Table 2). When accounting for trunks, WAD ranged from 0.014 to 0.036.

Estimates of the clumping coefficient

Under the spherical assumption for leaf angle distribution, the two trees that were never pruned (R1 and R4) showed radically different behaviours (Table 2): tree R1 had a clear foliage clumping ($\mu = 0.56$) whereas tree R4 seemed to have a very regular leaf distribution ($\mu = 4.90$). However, these trees had very low-hanging branches that caused two problems in the analysis of hemispherical photographs: (i) the gap fraction values measured from photographs with tree leaves very close to the camera are unstable and unreliable: a leaflet close to the camera will obscure a large amount of the sky vault. Using these pictures for estimating the clumping coefficient leads to artificially high and unstable values for μ; (ii) for such unpruned trees, the silhouettes of neighbour trees are intimately mixed with the silhouette of the studied tree, leading to an additional uncertainty in the relationship between the estimated proportion of sky obscured on photographs and the distance from the tree.

The first problem explained that the very high μ observed for tree R4 was not significantly different from 1. The high apparent foliage clumping for tree R1 also resulted from an additional artifact: very low-hanging branches of this tree led to the parameterization of an ellipsoid touching the soil (Table 1). As

Table 2 Estimated values and confidence intervals for μ and WAD

Tree	Estimation of WAD (m^2 m^{-3})		Estimation of μ after computation of WAD with trunks	
	Without trunks	With trunks	Spherical $G(\Omega)$	Explicit $G(\Omega)$
R1	0.023 ± 0.002	0.020 ± 0.002	0.56 ± 0.11	0.39 ± 0.11
R2	0.036 ± 0.006	0.014 ± 0.001	0.80 ± 0.05	0.52 ± 0.03
R3	0.045 ± 0.006	0.017 ± 0.002	0.99 ± 0.14	0.65 ± 0.09
R4	0.039 ± 0.003	0.033 ± 0.003	4.90 ± NA	3.42 ± NA
N1	0.048 ± 0.002	0.030 ± 0.002	0.47 ± 0.03	0.32 ± 0.03
N2	0.049 ± 0.004	0.027 ± 0.003	0.53 ± 0.06	0.35 ± 0.04
N3	0.059 ± 0.006	0.036 ± 0.003	1.15 ± 0.23	0.76 ± 0.15
N4	0.048 ± 0.005	0.029 ± 0.003	1.21 ± 0.16	0.81 ± 0.10
All trees but R1 and R4	0.048 ± 0.003	0.026 ± 0.002	0.76 ± 0.06	0.50 ± 0.04

The parameters were estimated from least square regression from winter photographs for WAD and summer photographs for μ. Parameters were either estimated from photographs taken under one tree or from all photographs excepted those from trees R1 and R4. For tree R4, the confidence interval of the very large value of μ was not computable by the R nls method

a consequence, some photographs were shot from locations that laid inside the adjusted ellipsoid. For these photographs, all rays in the model are intercepted by the tree, leading to a more than 90% shaded fraction under the no clumping hypothesis, whereas picture analysis leads to values ranging from 65 to 85%. This resulted in the estimation of a very low and unreliable clumping coefficient.

For these reasons, the two unpruned trees R1 and R4 were not used for cross validation and evaluation of the model.

The clumping coefficient estimated with the other trees ranged from 0.47 (tree N1) to 1.15 (tree N3) with the spherical leaf angle distribution, and from 0.32 to 0.81 with the explicit leaf angle distribution. In both cases, the large pruned trees (R3, N3, N4 and R2) had a larger μ than small trees (N1 and N2), suggesting a more regular leaf distribution.

Model evaluation

Predicting the shaded fraction under leafless trees

By construction, the null model (without trunks nor branches) is unable to predict any sky mask by leafless trees. Accounting for light interception by trunks only was not sufficient for predicting the shaded fraction P under leafless trees (Table 3a). Estimating WAD

Table 3 Model evaluation with leafless trees: comparing the predicted shaded fraction P with hemispherical photographs

Tree	a			b			c			d		
	rB (%)	RMSrE (%)	EF	rB (%)	RMSrE (%)	EF	rB (%)	RMSrE (%)	EF	rB (%)	RMSrE (%)	EF
R2	46	48	≈0	ns	−61	0.76	−49	52	0.06	−2	9	0.95
R3	45	48	<0	6	−25	0.47	−27	34	0.61	−1	16	0.90
N1	72	74	<0	−27	−5	0.11	−16	22	0.92	6	16	0.97
N2	66	69	<0	−26	−8	0.23	8	19	0.90	5	18	0.91
N3	66	67	<0	10	15	0.23	22	24	0.49	−2	11	0.90
N4	66	67	<0	14	−12	0.26	7	11	0.91	−2	9	0.95
All	59	62	<0	−1	−17	0.43	−6	31	0.75	ns	13	0.95

(a) Model accounting for trunks only. (b) Interception by trunks was not explicitly computed, WAD was estimated from 5 trees and model evaluated on the 6th. (c) Model accounting for trunks, WAD was estimated from 5 trees and model evaluated on the 6th. (d) Model accounting for trunk, WAD was estimated from 1 tree and model evaluated on the same tree. rB, RMSrE and EF are the relative bias (Eq. 6), the root mean squared relative error (Eq. 7), and the model efficiency (Eq. 8)

ns signifies smaller than 0.5%

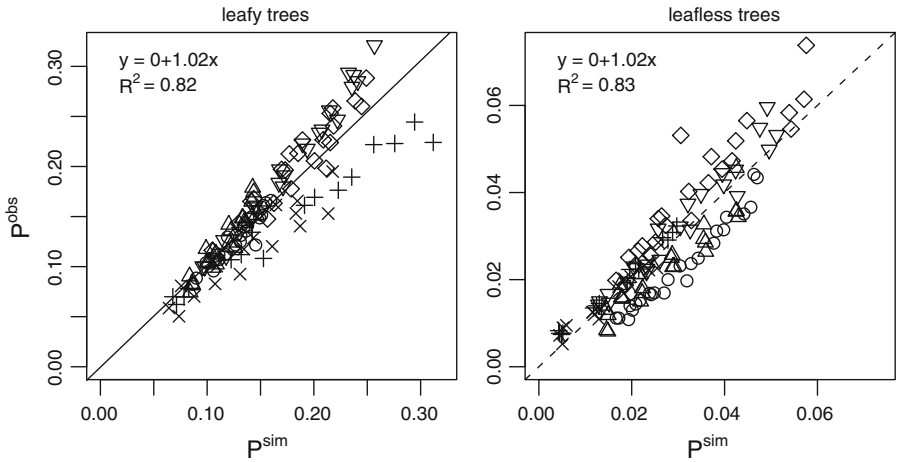

Fig. 4 Simulated versus observed shaded fraction P on hemispherical photographs, with the model including light interception by trunk, and both parameters μ and WAD estimated from all trees, leaf angle distribution was kept spherical. Each *point* represents an hemispherical photograph, with symbols ^, Δ, +, × , ◇ and ▽ for trees R2, R3, N1, N2, N3 and N4 respectively

and evaluating the model on the same tree (Table 3d) informs about the best prediction that is attainable for each tree without changing the model formalisms (ellipsoids for tree crowns, cones for trunks). For all trees, our model can predict P with a small bias (rB $< 6\%$) and a greater than 0.9 efficiency.

When the wood area density was estimated from other trees (cross validation), the explicit interception by conical trunks improved the model performances for all trees (Table 3b vs. c), reducing the bias (rB $= 6\%$) and improving the efficiency (EF $= 0.75$, see Fig. 4) on the whole dataset (all trees). However, the model was poorly performant when evaluated on individual trees: P was for example under-estimated by 49% for tree R2 while it was over-estimated by 22% for tree N3.

Predicting the shaded fraction by leafy trees

Introducing light interception by branches and stems had very few effects on model evaluation under leafy trees (results not shown). Global predictions (on all trees) of the model without clumping ($\mu = 1$) and a spherical $G(\Omega)$ showed good agreement between observed (P^{obs}) and simulated (P^{sim}) shaded fractions (Table 4a), with a 11% relative bias and an efficiency of 0.74. However tall and small trees behaved differently: the model gave proper estimates for tall trees (R2, R3, N3 and N4)—the relative bias was low with 1% underestimations to 9% overestimations, the RMSrE was about 10% and the model efficiency exceeded 0.7—while the shaded fraction was over-estimated by more than 30% for small trees (N1 and N2), resulting in a poor predictive power (EF < 0).

The model with an explicit leaf angle distribution and no leaf clumping largely overestimated P for all trees, and the details of its evaluation are not presented. When μ was estimated and the model used on the same tree (Table 4d with the explicit leaf angle distribution; note that the spherical leaf angle distribution gave very similar results), predictions of P were not biased and very efficient (EF > 0.8) for all trees, showing that our formalism is able to reproduce the spatial variability of P under individual trees. However, the value of RMSrE (about 10%) suggests that using simple ellipsoids does not allow a good reproduction of all the variability observed with hemispherical photographs.

Introducing an average clumping coefficient deduced from other trees increased little the model performance (Table 4b,c), whatever the assumption for the leaf angle distribution was. The overestimation of P was reduced from 11% to less than 1%, but efficiency was unchanged and RMSrE little reduced.

These results indicate that while introducing a clumping coefficient could theoretically increase the model accuracy, this may not prove correct. This coefficient was too variable between trees and using a single average value was not efficient to increase the model performances. We finally will use the

Table 4 Model evaluation under leafy trees: comparing the predicted shaded fraction P with hemispherical photographs

Tree	a			b			c			d		
	rB (%)	RMSrE (%)	EF	rB (%)	RMSrE (%)	EF	rB (%)	RMSrE (%)	EF	rB (%)	RMSrE (%)	EF
R2	−9	11	0.7	ns	6	0.90	1	6	0.90	−1	6	0.90
R3	−3	10	0.84	6	10	0.72	6	10	0.74	−2	10	0.84
N1	−33	35	<0	−27	29	0.30	−25	27	0.37	04	10	0.96
N2	−38	41	<0	−26	31	0.34	−25	29	0.35	ns	12	0.89
N3	1	8	0.89	10	12	0.68	9	12	0.70	−1	8	0.90
N4	1	8	0.92	14	16	0.63	14	16	0.65	−3	8	0.95
all	−11	21	0.74	−1	18	0.73	ns	17	0.74	ns	9	0.96

(a) Spherical leaf angle distribution, no leaf clumping ($\mu = 1$). (b) Spherical leaf angle distribution, μ estimated from 5 trees and model evaluated on the sixth. (c) Explicit leaf angle distribution, μ estimated from 5 trees and model evaluated on the sixth. (d) Explicit leaf angle distribution, μ estimated from 1 tree and model evaluated on the same tree. In all cases, the model included interception by trunks (approximated as opaque cones) and branches (WAD = 0.026 m^2 m^{-3})

ns signifies smaller than 0.5 %

value $\mu = 0.76$ estimated from all trees under the spherical leaf angle distribution assumption as a reference for the sensitivity analysis. Predicted versus observed values for the shaded fraction are plotted in Fig. 4.

Sensitivity analysis

Light capture efficiency of trees

The light capture efficiency ε of trees provides information about the sum of self-shading within trees and light competition between trees (Fig. 5a). In the low density plot (15 × 15 m), ε was similar for large and small trees, indicating similar self-shading rates: the crown size of large trees is compensated by a lower leaf area density. ε is little affected by light competition in the high density plot for small trees (−3%) while it is reduced by 20% for large trees. Light capture efficiency is very sensitive to μ (Table 5), with elasticities ranging from 0.42 to 0.51, but insensitive to WAD. Even for large trees in the high density plot, the elasticity of WAD is only −0.02, indicating that modelling light interception by branches is useless when focussing on light interception by leafy trees.

PAR transmittance under leafy trees

Whatever the values for μ and WAD, the amount of PAR intercepted on the large plot by small trees in our simulations was little compared to the total PAR incident, so that the PAR transmittance on the plot remained close to 1 (Fig. 5b) and was little sensitive to μ and WAD (Table 5). For large trees, the PAR transmittance was reduced and more sensitive to μ, with elasticities of 0.18 and 0.76 for trees planted at 15 and 9 m spacing respectively. WAD values can affect the PAR transmittance under large trees, but sensitivity to WAD remained negligible relatively to sensitivity to μ.

PAR transmittance under leafless trees

PAR interception by leafless small trees was negligible at the plot level, whatever the plot density and the parameters values (Fig. 5c): less than 3% of incident PAR were intercepted by trees. On the contrary, branches and trunks of large trees intercepted 12 and 29% of the incident PAR and had elasticities of −0.28 and −0.10 (Table 5) in the low and high density plots respectively.

Discussion

Should we account for light interception by branches and stems?

The sensitivity analysis showed that accounting for light interception by woody elements had a negligible effect on the predicted light capture efficiency and transmittance for leafy trees. This is consistent with the fact that it is neglected by most simple light

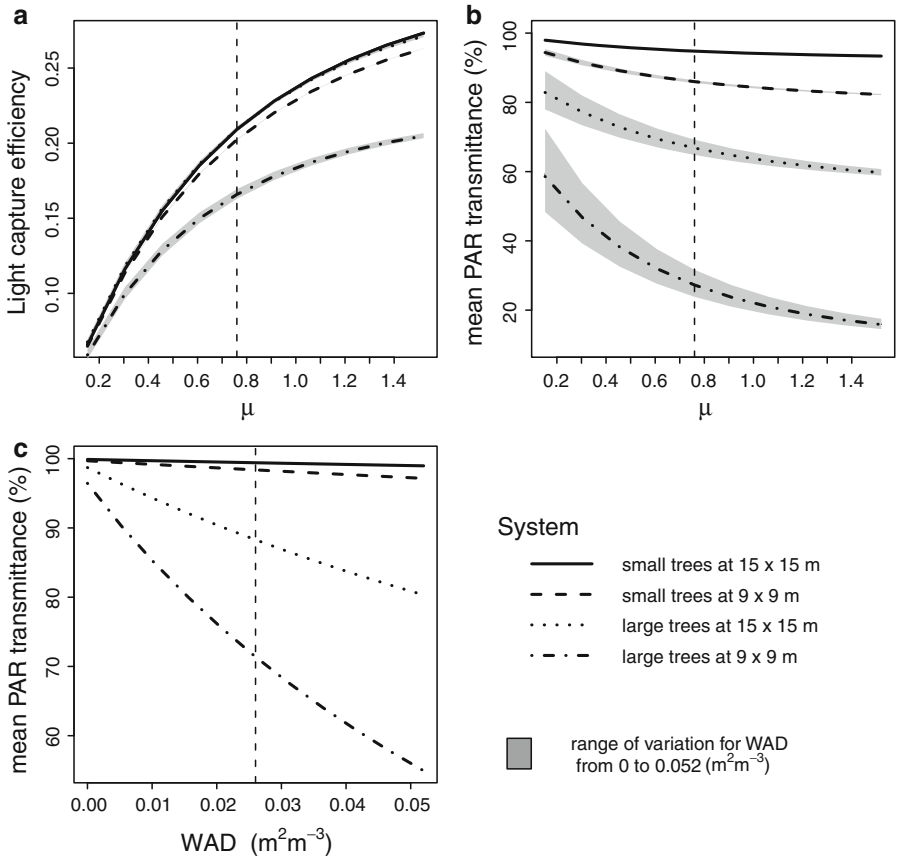

Fig. 5 Sensitivity of three model outputs to parameters μ and WAD for small (5m high, $r_x = r_y = 1.9$ m, $r_z = 1.8$ m, LAD = 1.5) or large (15m high, $r_x = r_y = 4.5$m, $r_z = 5.6$m, LAD = 0.51) trees planted at 9m or 15m spacing. **a** Light capture efficiency (ε, averaged over the leafy period). **b** PAR transmittance under leafy trees. **c** PAR transmittance under leafless trees (only to the wood area density WAD). The PAR transmittance was averaged over the simulated plot and during the leafy (from 15/04 to 15/11) or leafless (rest of the year) period

Table 5 Elasticity of the model predictions to parameters μ and WAD for model predictions

Analysed output	Parameter	Large trees		Small trees	
		9 m	15 m	9 m	15 m
Light capture efficiency	μ	0.42	0.50	0.50	0.51
	WAD	−0.02	−0.01	ns	ns
Summer PAR transmittance	μ	−0.76	−0.18	−0.07	−0.02
	WAD	−0.14	−0.03	ns	ns
Winter PAR transmittance	WAD	−0.28	−0.10	−0.01	ns

Elasticities are computed at the parameter values estimated from all trees for the model accounting for trunks and assuming a spherical leaf angle distribution ($\mu = 0.76$, WAD = 0.026)

ns signifies lower than 0.005

models designed for forest or orchard stands (Zhao et al. 2003; Oyarzun et al. 2007). However, in the case of agroforestry systems with phenological lags between deciduous trees and winter crop species, the prediction of light availability under a leafless tree canopy is important. According to our simulations, in a stand of 15 m tall walnut trees at 156 trees ha^{-1}, winter PAR transmittance is reduced by 29% by leafless trees (Fig. 5). Such a reduction in PAR availability can reduce drastically the crop productivity (Li et al. 2008), as winter radiation levels are already very low. This impact was never cited in the agroforestry literature nor included in agroforestry light models.

When the model was evaluated on the whole dataset of hemispherical pictures for all the trees, we

obtained unbiased and efficient predictions (Table 3c, Fig. 4) of the proportion P of sky obscured by leafless trees by introducing a wood area density parameter estimated from other trees, and by using a simple description of stems by cones as proposed by Brunner (1998). This was validated with hemispherical photographs data. The model is thus able to globally reproduce the spatial pattern of irradiance at ground level for various tree sizes. However, the poor performances of the model when evaluated on individual trees indicated that an average wood area density cannot reproduce the effects of architectural specificities of trees. The model can only be used to predict the average shade pattern under an average tree, but this is what is usually expected from an agroforestry model.

Should we take leaf clumping within crown into account?

The clumping coefficient, when estimated at the single shoot scale, may be related to botanical parameters (Falster and Welstoby 2003). When it is estimated at larger scales, it integrates different levels of clumping that may compensate. In our study case, it included the clumping at shoot and tree scale, clumping at stand scale being explicitly taken into account by modelling the crowns of individual trees. Parveaud et al. (2008) checked the influence of the random leaf area distribution ($\mu = 1$) hypothesis at different scales on light interception with 3D detailed mock-ups of young hybrid walnuts describing the trees at the leaf scale. They concluded that the random hypothesis held at the shoot scale, but led to an over-estimation of the intercepted light at the branch or the whole crown scale. They also showed that using a spherical leaf angle distribution led to an under-estimation of the intercepted light. Our results indicate that the issue is more complicated when the trees are approximated by simple ellipsoids, the μ estimate being dependent from the procedure to adjust the ellipsoid.

Light models that simplify tree canopies with simple volumes such as cones, cylinders or ellipsoids are sensitive to the procedure to adjust these volumes and to their optical parameters (Stadt and Lieffers 2000; Zhao et al. 2003; Mõttus et al. 2006). Trees have inherently a complex shape, and numerous geometric shapes and calibration procedures can approximate a real tree canopy shape. For a stand of young grey alders (*Alnus incana*) approximated by ellipsoids, Mõttus et al. (2006) concluded that the optimal calibration procedure for modelling light transmittance should end up with ellipsoids including 95% of the leaves. This conclusion was obtained with 3D mock-ups of the trees and involved heavy workload. Therefore, it is not advisable as an easy parameterization procedure of ellipsoids. In this paper, we explored a simpler procedure, easy to reproduce, and requiring only few input data. All state variables used by the model to describe the tree canopy depend on this procedure, such as the volume and coordinates of the adjusted ellipsoid and the mean leaf area density within this volume. As a consequence, as stated by Cescatti (1997b), the clumping coefficient defined at the tree scale is more a fitting than a bio-physically meaningful parameter. It accounts both for leaf clumping at shoot and tree scale and for discrepancies between real trees and adjusted ellipsoids: any intercepting surface (isolated leafy branches, tree trunk) situated outside the adjusted ellipsoid tends to increase μ, while zones empty of leaves in the adjusted ellipsoid tend to decrease it.

The clumping parameter ranged from 0.47 to 1.21 for our six hybrid walnut trees assuming a spherical leaf angle distribution. It was close to 0.5 with a small confidence interval for small trees, while it ranged from 0.8 to 1.2 with much larger confidence intervals for large pruned trees (Table 2). This results from a poor agreement between the actual crown shape of large trees and ellipsoids. As a consequence, introducing an average clumping coefficient estimated from other trees was inefficient for improving the predicted shade fraction around individual trees. Therefore, more detailed light modelling around a given tree could only be achieved with a more detailed crown description of that tree. Nevertheless, the model evaluation on the whole dataset showed that it captured the main effects of tree size and photograph positions on the shaded fraction ($EF = 0.73$, $R^2 = 0.82$), and that introducing a correcting clumping coefficient reduced the bias of model predictions. As a conclusion, μ can be used as a correcting parameter only if specific data are available, which is not the case for most situations were generic models are used.

Accuracy of model predictions

The global evaluation of the model showed that it captured most of the variability of the shaded fraction on hemispherical pictures taken at various positions under leafy or leafless trees of various size (Fig. 4). The model is thus adapted for rendering the spatial heterogeneity and dynamics during various stages of the life of trees for the shaded fraction at soil level under a virtual stand of average trees. However, when the evaluation was performed tree by tree, we obtained overestimates for some trees, underestimates for others, with a large RMSrE: our model is not adapted to take into account the effects of architectural specificities of a given tree, and should be applied only to an average virtual tree. This aspect was ignored by most previous papers addressing this issue (Courbaud et al. 2003; Bartelink 1998; Zhao et al. 2003). It cannot be ignored when using the model on a specific tree such as a real tree that would be monitored in a field tree-crop interaction study.

The sensitivity analysis gave us information about the uncertainty of model predictions for PAR capture efficiency by trees and PAR transmittance under trees at different age and density. This will be useful in the construction of an integrated wide-spaced tree stand (agroforestry, orchard, urban forestry) model. It will set the requirements for the level of precision that should be expected from the other modules that will be included in the integrated model.

Using gap-inversion methods for estimating canopy parameters of wide-spaced trees

To our knowledge, the reported use of hemispherical photographs in a spatially explicit context is scarce. Fournier et al. (1996), Parveaud et al. (2008) and Stuckens et al. (2009) used hemispherical photographs to evaluate spatially explicit light models and/or methods for reconstructing individual tree architecture. Courbaud et al. (2003) used hemispherical photographs for the calibration of the LAD and the evaluation of a light model for norway spruce stands. In this paper, we proposed a method for estimating structural parameters of individual trees by inversion of the shaded-fraction on hemispherical photographs with a spatially explicit radiation interception model. The advantages and pitfalls of gap-fraction inversion methods have been extensively discussed (Jonckheere et al. 2004), and several theories and softwares have been developed to improve the image processing (Jonckheere et al. 2005; Cescatti 2007), to account for horizontal heterogeneity (Nilson 1999), leaf clumping at several scales (Cohen et al. 1995) or multiple scattering (Leblanc and Chen 2001). With the notables exeptions of the work of Phattaralerphong et al. (2008) and Zhao et al. (2003) with classical photographs, Villalobos et al. (1995) with a Plant Canopy Analyzer (LI-COR LAI 2000) and Huang and Pretzsch (2010) with a terrestrial laser, most of these methods were designed for studies at the whole canopy scale with no spatially explicit description, and are not suitable to predict the radiation heterogeneous pattern at ground (or crop) level.

Conclusions

We have developed a simple yet spatially explicit model for predicting light competition in wide-spaced tree stands such as those observed in savannahs, orchards, agroforestry systems and urban forestry. Predicting the spatial patterns of light availability at ground level is required for the modelling of microclimate and productivity of the understorey. Spatially heterogeneous levels of radiation may induce heterogeneity in the understorey that could be detrimental to productivity. As an example, this could perhaps prevent certain crops to perform economically within agroforestry systems. Accurately predicting the light availability and heterogeneity at ground or crop level in wide-spaced tree stands is therefore crucial. This model uses well established theories of light interception by heterogeneous canopies and uses a canopy description at the scale of an individual tree crown. We tested if introducing parameters that account for light interception by woody elements and non random leaf distribution would improve the accuracy of prediction of the model. The parameterization of a wood area density improved the model, providing unbiased predictions of the shaded fraction under leafless trees, and slightly improved predictions of the spatial light heterogeneity at crop level. Surprisingly, the introduction of a clumping coefficient failed to improve model predictions for leafy trees. Although this improvement of light competition models was suggested by several authors, our study indicates that the estimation of the clumping coefficient was too

dependent of the canopy volume adjustment procedure. This procedure was not efficient enough to account for the actual shape of individual tree crowns. Our conclusions back the use of a simple light interception model to simulate the day to day variation of light interception by discontinuous canopies of spaced trees provided that the model aims at predicting the impact of an average tree. Predicting the detailed light interception by a real tree is not within the reach of any simplified model that assimilates the tree crown to an ellipsoid.

References

Annandale JG, Jovanovic NZ, Campbell GS, Sautoy Nd, Lobit P (2004) Two-dimensional solar radiation interception model for hedgerow fruit trees. Agric For Meteorol 121:207–225. doi:10.1016/j.agrformet.2003.08.004

Bartelink H (1998) Radiation interception by forest trees: a simulation study on effects of stand density and foliage clustering on absorption and transmission. Ecol Model 105:213–225. doi:10.1016/S0304-3800(97)00165-8

Begué A, Prince S, Hanan N, Roujean J (1996) Shortwave radiation budget of sahelian 2. radiative transfer models vegetation. Agric For Meteorol 79:97–112. doi:10.1016/0168-1923(95)02269-4

Bonhomme R (1993) The solar radiation: characterization and distribution in the canopy. In: Varlet-Granchet C, Bonhomme R, Sinoquet H (eds) Crop structure and light microclimate. INRA, Paris, pp 17–28

Brisson N, Mary B, Ripoche D, Jeuffroy M, Ruget F, Nicoullaud B, Gate P, Devienne-Barret F, Antonioletti R, Durr C, Richard G, Beaudoin N, Recous S, Tayot X, Plenet D, Cellier P, Machet J, Meynard J, Delecolle R (1998) Stics: a generic model for the simulation of crops and their water and nitrogen balances. 1. Theory and parameterization applied to wheat and corn. Agronomie 18:311–346. doi:10.1051/agro:2001005

Brunner A (1998) A light model for spatially explicit forest stand models. For Ecol Manag 107:19–46. doi:10.1016/S0378-1127(97)00325-3

Casella E, Sinoquet H (2007) Botanical determinants of foliage clumping and light interception in two-year-old coppice poplar canopies: assessment from 3-d plant mock-ups. Ann For Sci 64:395–404. doi:10.1051/forest:2007016

de Castro F, Fetcher N (1998) Three dimensional model of the interception of light by a canopy. Agric For Meteorol 90:215–233. doi:10.1016/S0168-1923(97)00097-X

de Castro F, Fetcher N (1999) The effect of leaf clustering in the interception of light in vegetal canopies: theoretical considerations. Ecol Model 116:125–134. doi:10.1016/S0304-3800(98)00170-7

Cescatti A (1997a) Modelling the radiative transfer in discontinuous canopies of asymmetric crowns. I. model structure and algorithms. Ecol Model 101:263–274. doi:10.1016/S0304-3800(97)00050-1

Cescatti A (1997b) Modelling the radiative transfer in discontinuous canopies of asymmetric crowns. II. Model testing and application in a norway spruce stand. Ecol Model 101:275–284. doi:10.1016/S0304-3800(97)00055-0

Cescatti A (2007) Indirect estimates of canopy gap fraction based on the linear conversion of hemispherical photographs: methodology and comparison with standard thresholding techniques. Agric For Meteorol 143:1–12. doi:10.1016/j.agrformet.2006.04.009

Chen J (1996) Optically-based methods for measuring seasonal variation of leaf area index in boreal conifer stands. Agric For Meteorol 80:135–163. doi:10.1016/0168-1923(95)02291-0

Cohen S, Mosoni P, Meron M (1995) Canopy clumpiness and radiation penetration in a young hedgerow apple orchard. Agric For Meteorol 76:185–200. doi:10.1016/0168-1923(95)02226-N

Courbaud B, de Coligny F, Cordonnier T (2003) Simulating radiation distribution in a heterogeneous norway spruce forest on a slope. Agric For Meteorol 116:1–18. doi:10.1016/S0168-1923(02)00254-X

Dauzat J, Rapidel B, Bergé A (2001) Simulation of leaf transpiration and sap flow in virtual plants: model description and application to a coffee plantation in costa rica. Agric For Meteorol 109:143–160. doi:10.1016/S0168-1923(01)00236-2

Dupraz C, Newman S (1997) Temperate agroforestry: the european way. In: Gordon AM, Newman S (eds) Temperate agroforestry systems. CAB International, UK, pp 181–236

Falster D, Welstoby M (2003) Leaf size and angle vary widely across species: what consequences for light interception. New Phytol 158:509–525. doi:10.1046/j.1469-8137.2003.00765.x

Fournier R, Landry R, August N, Fedosejevs G, Gauthier R (1996) Modelling light obstruction in three conifer forests using hemispherical photography and fine tree architecture. Agric For Meteorol 82:47–72. doi:10.1016/0168-1923(96)02345-3

Frazer G, Canham C, Lertzman K (1999) Gap light analyser (GLA): imaging software to extract canopy structure and gap light transmission indices from true-colour Fisheye photographs. Users manual and program documentation, Version 2.0. Simon Fraser University, Burnaby, British Columbia

Goudriaan J (1977) Crop micrometeorology: a simulation. Wageningen Centre for Agricultural Publishing and Documentation, Wageningen

Huang P, Pretzsch H (2010) Using terrestrial laser scanner for estimating leaf areas of individual trees in a conifer forest. Trees 24:609–619. doi:10.1007/s00468-010-0431-z

Jonckheere I, Fleck S, Nackaerts K, Muysa B, Coppin P, Weiss M, Baret F (2004) Review of methods for in situ leaf area index determination. Part I. theories, sensors and hemispherical photography. Agric For Meteorol 121:19–35. doi:10.1016/j.agrformet.2003.08.027

Jonckheere I, Nackaerts K, Muys B, Coppin P (2005) Assessment of automatic gap fraction estimation of forests from digital hemispherical photography. Agric For Meteorol 132:96–114. doi:10.1016/j.agrformet.2005.06.003

Kho R, Yacouba B, Yayé M, Katkoré B, Moussa A, Iktam A, Mayaki A (2001) Separating the effects of trees on crops:

the case of *Faidherbia albida* and millet in niger. Agrofor Syst 52:219–238. doi:10.1023/A:1011820412140

Knyazikhin Y, Kranigk J, Miessen G, Panfyorov O, Vygodskaya N, Gravenhorst G (1996) Modelling three-dimensional distribution of photosynthetically active radiation in sloping coniferous stands. Biomass Bioenerg 11:189–200. doi:10.1016/0961-9534(96)00010-4

Lamanda N, Dauzat J, Jourdan C, Martin P, Malézieu E (2008) Using 3d architectural models to assess light availability and root bulkiness in coconut agroforestry systems. Agrofor Syst 72:63–74. doi:10.1007/s10457-007-9068-3

Leblanc S, Chen J (2001) A practical scheme for correcting multiple scattering effects on optical lai measurements. Agric For Meteorol 110:125–139. doi:10.1016/S0168-1923(01)00284-2

Li F, Meng P, Fu D, Wang B (2008) Light distribution, photosynthetic rate and yield in a paulownia-wheat intercropping system in china. Agrofor Syst 74(2):163–172. doi:10.1007/s10457-008-9122-9

Mõettus M, Sulev M, Lang M (2006) Estimation of crown volume for a geometric radiation model from detailed measurements of tree structure. Ecol Model 198:506–514. doi:10.1016/j.ecolmodel.2006.05.033

Mariscal M, Orgaz F, Villalobos F (2000) Modelling and measurement of radiation interception by olive canopies. Agric For Meteorol 100:183–197. doi:10.1016/S0168-1923(99)00137-9

Mariscal M, Marens S, Ustin S, Chen J, Weiss S, Roberts D (2004) Light-transmission profiles in an old-growth forest canpy: Simulation of photosynthetically active radiation by using spatially explicit radiative transfer models. Ecosyst 7:454–467. doi:10.1007/s10021-004-0137-4

Martens S, Breshears D, Meyer C (2000) Spatial distribution of understory light along the grassland/forest continuum: effect of cover, height, and spatial pattern of tree canopies. Ecol Model 126:79–93. doi:10.1016/S0304-3800(99)00188-X

Mialet-Serra I, Dauzat J, Auclair D (2001) Using plant architectural models for estimation of radiation transfer in a coconut-based agroforestry system. Agrofor Syst 53: 141–149. doi:10.1023/A:1013320419289

Moon P, Spencer D (1942) Illumination from a non-uniform sky. Trans Illum Eng Soc N Y 37:707–726

Mulia R, Dupraz C (2006) Unusual fine root distributions of two deciduous tree species in southern france: What consequences for modelling of tree root dynamics. Plant Soil 281:71–85. doi:10.1007/s11104-005-3770-6

Nair P (2007) The coming age of agroforestry. J Sci Food Agric 87:1613–1619. doi:10.1002/jsfa.2897

Nilson T (1971) A theoretical analysis of the frequency of gaps in plant stands. Agric Meteorol 8:25–38. doi:10.1016/0002-1571(71)90092-6

Nilson T (1999) Inversion of gap frequency data in forest stands. Agric For Meteorol 98(99):443–448. doi:10.1016/S0168-1923(99)00114-8

Norman JM, Welles JM (1983) Radiative transfer in an array of canopies. Agron J 75:481–488. doi:10.2134/agronj1983.00021962007500030016x

Oyarzun R, Stöckle C, Whiting M (2007) A simple approach to modeling radiation interception by fruit-tree orchards. Agric For Meteorol 142:12–24. doi:10.1016/j.agrformet.2006.10.004

Parveaud CE, Chopard J, Dauzat J, Courbaud B, Auclair D (2008) Modelling foliage characteristics in 3d tree crowns: influence on light interception and leaf irradiance. Trees 22:87–104. doi:10.1007/s00468-007-0172-9

Phattaralerphong J, Sathornkich J, Sinoquet H (2008) A photographic gap fraction method for estimating leaf area of isolated trees: assessment with 3D digitized plants. Tree Physiol 26:1123–1136. doi:10.1093/treephys/26.9.1123

Reisner Y, Filippi Rd, Herzog F, Palma J (2007) Target regions for silvoarable agroforestry in europe. Ecol Eng 29(4): 401–418. doi:10.1016/j.ecoleng.2006.09.020

Roupsard O, Dauzat J, Nouvellon Y, Deveau A, Feintrenie L, Saint-André L, Mialet-Serra I, Braconnier S, Bonnefond J, Berbigier P, Epron D, Jourdan C, Navarro M, Bouillet J (2008) Cross-validating sun-shade and 3d models of light absorption by a tree-crop canopy. Agric For Meteorol 148:549–564. doi:10.1016/j.agrformet.2007.11.002

Sinoquet H, Sonohat G, Phattaralerphong J, Godin C (2005) Foliage randomness and light interception in 3-d digitized trees: an analysis from multiscale discretization of the canopy. Plant Cell Environ 28:1158–1170. doi:10.1111/j.1365-3040.2005.01353.x

Sinoquet H, Stephen J, Sonohat G, Lauri P, Monney P (2007) Simple equations to estimate light interception by isolated trees from canopy structure features: assessments with three-dimensional digitized apple-trees. New Phytol 175:94–106. doi:10.1111/j.1469-8137.2007.02088.x

Stadt K, Lieffers V (2000) Mixlight: a flexible light transmission model for mixed-species forest stands. Agric For Meteorol 102:235–252. doi:10.1016/S0168-1923(00)00128-3

Stuckens J, Somers B, Delalieux S, Verstraeten WW, Coppin P (2009) The impact of common assumptions on canopy radiative transfer simulations: a case study in Citrus orchards. J Quant Spectrosc Radiat Trans 110:1–21. doi:10.1016/j.jqsrt.2008.09.001

Thanisawanyangkura S, Sinoquet H, Rivet P, Crétenet P, Jallas E (1997) Leaf orientation and sunlit leaf area distribution in cotton. Agric For Meteorol 86:1–15. doi:10.1016/S0168-1923(96)02417-3

Villalobos FJ, Orgaz F, Mateos L (1995) Non-destructive measurement of leaf area in olive (*Olea europaea* l.) trees using a gap inversion method. Agric For Meteorol 73:29–42. doi:10.1016/0168-1923(94)02175-J

Wang Y, Jarvis PG (1990) Description and validation of an array model: Maestro. Agric For Meteorol 51:257–280. doi:10.1016/0168-1923(90)90112-J

Zhao W, Qualls R, Berliner P (2003) Modeling of the short wave radiation distribution in an agroforestry system. Agric For Meteorol 118:185–206. doi:10.1016/S0168-1923(03)00108-4